

Synthesis of Fulvic Acid-Coated Magnetite ($\text{Fe}_3\text{O}_4\text{-FA}$) and Its Application for the Reductive Adsorption of $[\text{AuCl}_4]^-$

Philip Anggo Krisbiantoro, Sri Juari Santosa*, and Eko Sri Kunarti

Department of Chemistry, Faculty of Mathematics and Natural Sciences, Universitas Gadjah Mada, Sekip Utara, Yogyakarta 55281, Indonesia

Received May 5, 2017; Accepted July 10, 2017

ABSTRACT

Fulvic acid-coated magnetite ($\text{Fe}_3\text{O}_4\text{-FA}$) has been synthesized through coprecipitation method using NH_4OH . Synthesis of $\text{Fe}_3\text{O}_4\text{-FA}$ was conducted by cheap and environmentally friendly preparation used iron salts and extracted fulvic acid (FA) from Peat soil of Rawa Pening, Central Java, Indonesia. Characterization using FT-IR indicated that the coating of FA on Fe_3O_4 occurred through the formation of chemical bond between iron of Fe_3O_4 and carboxyl group of FA. The XRD measurement indicated that coated Fe_3O_4 successfully dispersed in smaller size than uncoated Fe_3O_4 , i.e. from 16.67 to 14.84 nm for Fe_3O_4 and $\text{Fe}_3\text{O}_4\text{-FA}$, respectively. Synthesized $\text{Fe}_3\text{O}_4\text{-FA}$ has pH_{PZC} 6.37 and stable at $\text{pH} > 3.0$. The extracted FA has total acidity 866.61 cmol kg^{-1} , $-\text{COOH}$ content 229.77 cmol kg^{-1} and $-\text{OH}$ content 636.84 cmol kg^{-1} . $\text{Fe}_3\text{O}_4\text{-FA}$ has total acidity 494.86 cmol kg^{-1} , $-\text{COOH}$ content 67.80 cmol kg^{-1} and $-\text{OH}$ content 427.06 cmol kg^{-1} . The adsorption rate constant (k) of $[\text{AuCl}_4]^-$ on $\text{Fe}_3\text{O}_4\text{-A}$ according to the Ho kinetic model was 8006.53 $\text{g mol}^{-1} \text{min}^{-1}$. The adsorption capacity (q_{max}) according to Langmuir isotherm model was $1.24 \times 10^{-4} \text{ mol g}^{-1}$. The presence of reduction towards the adsorbed $[\text{AuCl}_4]^-$ was shown by the appearance of peaks at 2θ : 37.41; 43.66; 64.25, and 76.67° in the XRD diffractogram.

Keywords: magnetite; fulvic acid; gold; adsorption; reduction

ABSTRAK

Telah dilakukan sintesis magnetit terlapisi asam fulvat ($\text{Fe}_3\text{O}_4\text{-AF}$) dengan metode kopresipitasi menggunakan NH_4OH . Sintesis $\text{Fe}_3\text{O}_4\text{-AF}$ telah dilakukan dengan menggunakan metode yang murah dan ramah lingkungan menggunakan garam besi dan asam fulvat yang diekstraksi dari tanah gambut Rawa Pening, Jawa Tengah, Indonesia. Pelapisan Fe_3O_4 oleh AF berhasil dilaksanakan berkat adanya ikatan antara besi pada Fe_3O_4 dan gugus karboksil pada FA sebagaimana ditunjukkan oleh spektra FT-IR. Karakterisasi dengan XRD menunjukkan bahwa Fe_3O_4 terlapisi lebih terdispersi dan memiliki ukuran lebih kecil daripada Fe_3O_4 tanpa pelapisan, secara berurutan ukuran Fe_3O_4 dan $\text{Fe}_3\text{O}_4\text{-AF}$ adalah 16,67 dan 14,84 nm. Hasil penelitian menunjukkan bahwa $\text{Fe}_3\text{O}_4\text{-AF}$ memiliki nilai pH_{PZC} 6,37 dan stabil pada $\text{pH} > 3,0$. AF hasil ekstraksi memiliki keasaman total 866,61 cmol kg^{-1} , kandungan gugus $-\text{COOH}$ total 229,77 cmol kg^{-1} dan kandungan gugus $-\text{OH}$ total 636,84 cmol kg^{-1} . $\text{Fe}_3\text{O}_4\text{-AF}$ memiliki keasaman total 494,86 cmol kg^{-1} , kandungan gugus $-\text{COOH}$ total 67,80 cmol kg^{-1} dan kandungan gugus $-\text{OH}$ total 427,06 cmol kg^{-1} . Konstanta laju reaksi (k) dengan model kinetika Ho adalah 8006,53 $\text{g mol}^{-1} \text{menit}^{-1}$. Kapasitas adsorpsi (q_{max}) dengan model isoterm Langmuir adalah $1,24 \times 10^{-4} \text{ mol g}^{-1}$. Logam Au hasil reduksi ditunjukkan dengan munculnya puncak 2θ : 37,41; 43,66; 64,25 dan 76,67° pada difraktogram XRD.

Kata Kunci: magnetit; asam fulvat; emas; adsorpsi; reduksi

INTRODUCTION

In recent years, large attention has been given to non-cyanide and mercury methods for gold recovery [1-6]. Non health threatening alternative approaches has widely been conducted by scientists [7], yet in comparison with cyanidation [8-11], most of alternative approaches are still uneconomical.

In the past decade, the synthesis of paramagnetic nanoparticles has been intensively developed, not only for scientific interest, but also for many technological

applications [12-13]. Especially in the field of adsorption, the dramatic increase on the use of magnetite as adsorbent for metal cations in waste water was observed [14-15]. However, magnetite is easily aggregated in aqueous solution and oxidized by free atmosphere [16]. Hence, surface modification is importantly needed to enhance the stability of magnetite nanoparticle [17].

Humic substances are the biggest type of organic matter present in biosphere and they also the most stable class than any other organic matter on earth

* Corresponding author. Tel : +62-274-545188
Email address : sjuari@ugm.ac.id

[18]. Due to short time of humification process, fulvic acid as the one of humic substance has higher total acidity instead of humic acid (HA) and humin [18]. Utilization of humic and fulvic acid includes removal of Cu(II), Zn(II), Mn(II), Fe(II), Pb(II), Cd(II), Cr(III), Cr(VI), Cr(III), and Cd(II), either through adsorption and photo-reduction [19-23].

Coating magnetite by HA has been widely reported as a heavy metals adsorbent in water [24]. As reported, coating of particle surface can effectively prevent the adhesion of colliding particles during thermal motion [25]. Recent studies also indicated that HA has high affinity to Fe_3O_4 particles and able to enhance the stability of nano dispersion of Fe_3O_4 particles by preventing their aggregation [25-27]. This surface modification of Fe_3O_4 by FA ($\text{Fe}_3\text{O}_4\text{-FA}$) increases adsorption capacity and easily separated from aqueous medium [25-27].

In this study, due to its highest total acidity which is highest than the other fractions of humic substances, FA is chosen to coat Fe_3O_4 and the formed $\text{Fe}_3\text{O}_4\text{-FA}$ is then applied to adsorb $[\text{AuCl}_4]^-$ in aqueous solution [28]. Skogerboe and Wilson [28] reported that fulvic acid had reduction potential approximately 0.5 V (vs normal hydrogen electrode), while the reduction potential of $[\text{AuCl}_4]^-$ is 0.1 V. Its means, reduction of $[\text{AuCl}_4]^-$ into Au(0) occur spontaneously. Higher total acidity needed in purpose to increase Fe_3O_4 stability. $\text{Fe}_3\text{O}_4\text{-FA}$ synthesized through coprecipitation method and characterized using FT-IR and XRD. Measurement of pH_{PZC} , Fe_3O_4 stability and total acidity were also investigated.

EXPERIMENTAL SECTION

Materials

Peat soil from Rawa Pening, analytical grade of NaOH, HCl 37%, $\text{Ba}(\text{OH})_2$, NH_4OH 25%, $\text{FeCl}_3 \cdot 6\text{H}_2\text{O}$, $\text{FeSO}_4 \cdot 7\text{H}_2\text{O}$, $\text{Ca}(\text{CH}_3\text{COO})_2$, NaNO_3 , HNO_3 , NaHCO_3 , $[\text{AuCl}_4]^-$, standard solution of Fe, were obtained from Merck (Germany) without further purification, distilled water from general laboratory of Chemistry Department (Universitas Gadjah Mada), and N_2 gas.

Instrumentation

Stirrer and hot plate (Nouva), analytical balance (Mettler Toledo AL204), centrifuge (K PLC series), electric pH-meter (Hanna Instrument 211), oven (Fischer Scientific model 655F), sieve 100 and 200 mesh, external magnetic field, shaker. Analytical instrumentals include infra-red spectrometer (Shimadzu FT-IR Prestige 21), atomic spectrometer (Perkin Elmer 3110),

UV-Vis spectrometer (Shimadzu UV-1700 Pharmaphec), X-ray diffractometer (Shimadzu XRD-6000).

Procedure

Extraction of fulvic acid

Peat soil was dried at room temperature and separated from roots and branches. Soil was crushed and sieved to pass through sieve of 100 mesh. The 100 g of sieved peat soil was added into 1.0 L of NaOH solution 1.0 M under stirring with N_2 atmosphere. The mixture was aged for 24 without stirring and then centrifuged at 4500 rpm for 30 min. After filtration, supernatant was added by HCl 6 M dropwise until pH 1 and followed by centrifugation at 4500 rpm for 30 min to precipitate HA. After separated from the precipitation, the supernatant was dried at 60 °C to solidify FA.

Synthesis of $\text{Fe}_3\text{O}_4\text{-FA}$

$\text{Fe}_3\text{O}_4\text{-FA}$ was synthesized with modified method from Ref. [30-31]. Briefly, $\text{FeSO}_4 \cdot 7\text{H}_2\text{O}$ (2.78 g) and $\text{FeCl}_3 \cdot 6\text{H}_2\text{O}$ (5.41 g) were dissolved in a 100 mL of distilled water. A 10 mL of NH_4OH 25% (v/v) and 1.0 g of FA were added into the mixed of $\text{Fe}^{2+}/\text{Fe}^{3+}$ solution at 90 °C under stirring, respectively. After aged for 30 min, the mixed solution was filtered and the separated solid was washed by distilled water until neutral pH and then dried at 60 °C to obtain $\text{Fe}_3\text{O}_4\text{-FA}$.

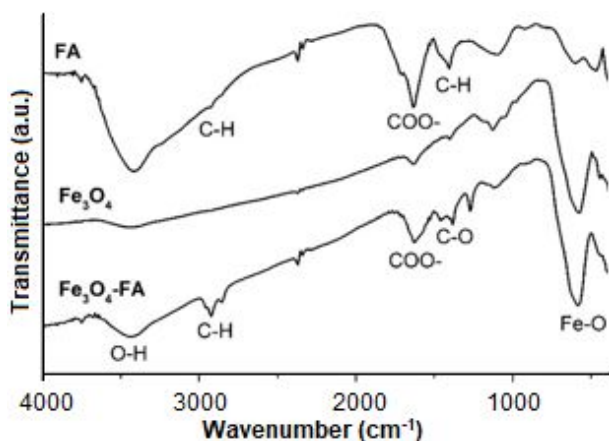
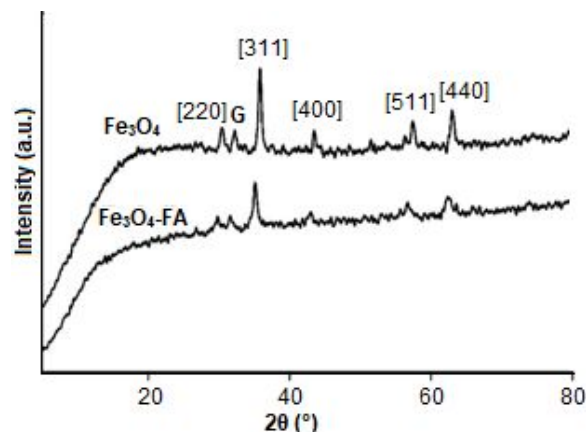
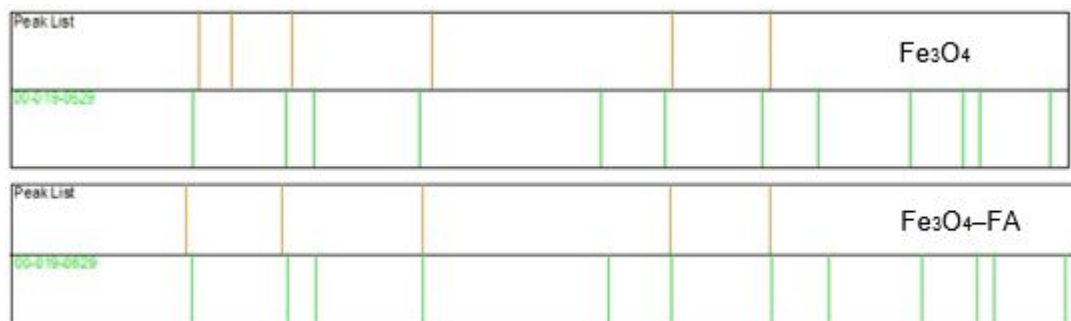
Determination of pH_{PZC} . $\text{Fe}_3\text{O}_4\text{-FA}$ (10 mg) was added into 10 mL of NaNO_3 0.01 M at various pH ranging from 2-12 by the addition of HNO_3 0.1 M or NaOH 0.1 M. The mixtures were shaken for 2 h and aged for 2 days. The filtrate was separated from solid by filtering using 0.45 μm paper and then final pH was measured.

Stability test. $\text{Fe}_3\text{O}_4\text{-FA}$ (10 mg) was added into 10 mL of distilled water at various pH ranging from 2-8 by addition of HCl 0.1 M or NaOH 0.1 M. The filtrate was separated from solid by filtering using 0.45 μm paper and then was analyzed its Fe content with AAS.

Adsorption of $[\text{AuCl}_4]^-$

The effect of pH. $\text{Fe}_3\text{O}_4\text{-FA}$ (10 mg) was added into a series of 10 mL of $[\text{AuCl}_4]^-$ solution 60 ppm at varies from 2 to 7. The mixture was shaken for 2 h and then the filtrate was separated by filtering using 0.45 μm paper and followed by analysis for the remaining $[\text{AuCl}_4]^-$ content with AAS.

Sorption kinetics. $\text{Fe}_3\text{O}_4\text{-FA}$ (10 mg) was added into a series of 10 mL of $[\text{AuCl}_4]^-$ at 60 ppm and optimum pH and each mixture was shaken at different contact time which ranges from 0 to 420 min. After filtering using

Fig 1. FT-IR spectra of FA, Fe₃O₄ and Fe₃O₄-FAFig 2. XRD diffractogram of FA, Fe₃O₄ and Fe₃O₄-FAFig 3. The comparison of Fe₃O₄ and Fe₃O₄-FA diffractogram to the JCPDS 00-019-0629**Table 1.** Size distribution and % crystallinity of Fe₃O₄ and Fe₃O₄-FA

Material	d ₃₁₁ (nm)	% crystallinity
Fe ₃ O ₄	16.67	100
Fe ₃ O ₄ -FA	14.84	62.22

0.45 μm filter paper, the filtrate was analyzed for its [AuCl₄]⁻ content by using AAS.

Sorption isotherm. Fe₃O₄-FA (10 mg) was added into a series of 10 mL of [AuCl₄]⁻ solution at various concentrations ranging from 5 to 250 ppm at optimum pH. The mixture was filtered using 0.45 μm filter paper and the filtrate was analyzed its [AuCl₄]⁻ content by using AAS.

RESULT AND DISCUSSION

Characterization of Adsorbent

FT-IR spectroscopy

Spectroscopic analysis showed the success of FA extraction from peat soil and coating onto Fe₃O₄ surface. As shown in Fig. 1, the IR spectra of FA possesses main absorption bands at 3410 cm⁻¹ for O-H stretching, 2931 cm⁻¹ for stretching of C-H aliphatic, 1635 cm⁻¹ for stretching of C=C aromatic and C=O carboxylic, and

1404 cm⁻¹ for the deformation of C-H aliphatic. This spectra of FA matched well with the obtained spectra of FA extracted from latosol soil by Jayaganesh and Senthurpandian [29]. The IR spectra of Fe₃O₄-FA displayed the main absorption bands at 1381 cm⁻¹ which correspond to C=O stretching of Fe₃O₄-FA, indicating the carboxylate anion in interaction with FeO surface, as the C=O in free carboxylic acid was above 1700 cm⁻¹ [25-27,30-31].

X-ray diffraction

The XRD measurement was used to identify the crystalline structure of the product. Fig. 2 indicates that Fe₃O₄-FA has diffraction pattern at 2θ = 29.81°; 35.12°; 42.89°; 56.62° and 62.30°, and slightly sifted than bare Fe₃O₄. The patterns sifted might due to synthesized Fe₃O₄ on Fe₃O₄-FA has smaller particles instead of bare Fe₃O₄ (Table 1). Decreasing intensity of Fe₃O₄-FA indicated that FA successfully coating the surface of Fe₃O₄. Both of Fe₃O₄ and Fe₃O₄-FA match well with the inverse cubic spinal structure of JCPDS 00-019-0629 (Fig. 3). This result indicated that the crystal structure of Fe₃O₄ was not change after coating by FA [25,32-33]. Fe₃O₄-FA has smaller size indicated that coated Fe₃O₄ successfully dispersed in smaller size instead of uncoated Fe₃O₄. Crystallinity percentage

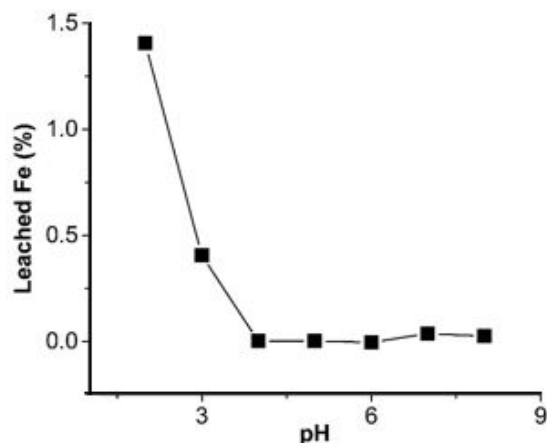
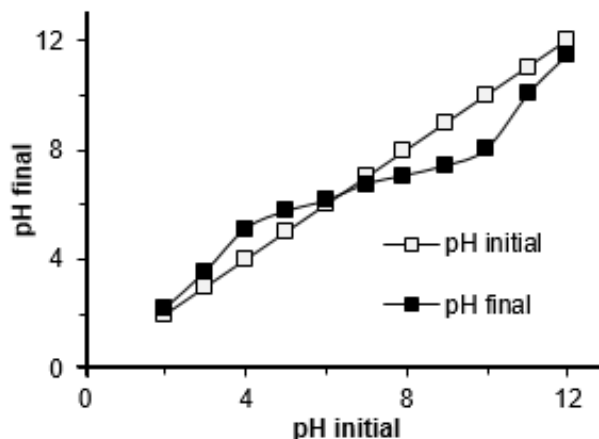
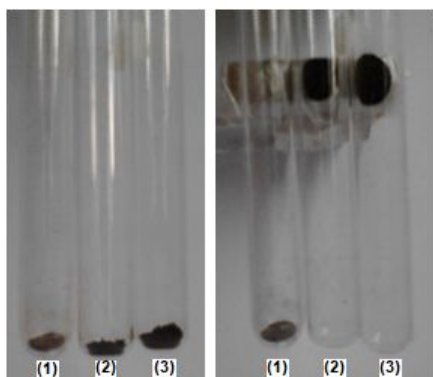


Fig 4. Leached Fe at various pH

Fig 5. The pH_{PZC} measurementFig 6. Qualitative magnetic properties test of fulvic acid (1); Fe₃O₄ (2) and Fe₃O₄-FA (3)Table 2. Functional groups of FA and Fe₃O₄-FA

Functional groups	Stevenson (cmol kg ⁻¹)	FA (cmol kg ⁻¹)	Fe ₃ O ₄ -FA (cmol kg ⁻¹)
Total acidity	570-890	866.61	494.86
-COOH	150-570	229.77	67.80
-OH	150-400	636.84	427.06

was also measured to compare the bare Fe₃O₄ and modified Fe₃O₄. By divided wide fraction of bare Fe₃O₄ and Fe₃O₄-FA, % crystallinity also can be determined, which FA decrease the % crystallinity of Fe₃O₄.

Functional groups of FA and Fe₃O₄-FA

The determination of total acidity and carboxyl content were carried out using Ba(OH)₂ and Ca-acetate method [34]. Table 2 shows that the functional groups of FA agreed well with Stevenson [34] and were decreased after coating the surface of Fe₃O₄, indicated that some of -COOH and -OH were used for bonding with Fe₃O₄ surface.

Stability test of Fe₃O₄-FA

Stability of Fe₃O₄-FA towards dissolution increased sharply from 2.0 to 4.0. At pH 2.0, Fe₃O₄ leached in the

solution was only 1.40% (2.51×10^{-5} mol g⁻¹) relative toward weight of the adsorbent (Fig. 4). At low pH, Fe²⁺ leached from adsorbent and form [Fe(H₂O)₆]²⁺ in the solution and detected as leached Fe by AAS. Meanwhile, the Fe₃O₄ that loses Fe²⁺ form maghemite (γ-Fe₂O₃) which has less magnetic properties instead of Fe₃O₄ [35]. The stability of Fe₃O₄ has high responsibility of the optimum pH of the adsorption process, which there is no possibility of the adsorbent could optimum at very low pH due to adsorbent stability. This concluded that Fe₃O₄-FA stable at pH > 3.0.

Determination of pH_{PZC} Value of Fe₃O₄-FA

The pH_{PZC} is a measurement of H⁺ ion movement onto and from the adsorbent surface [36]. The change of medium pH after aging adsorbent for 48 h is shown in Fig. 5. At low pH, H⁺ ions were moving from the solution onto adsorbent surface during aging and increase the pH of the solution. At high pH, H⁺ ions were moving from the adsorbent to the solution and decrease the pH of the solution. The meet point of initial and final pH mean that there is no movement of H⁺ ions and the adsorbent is about at neutral condition. The medium pH in which the H⁺ ions do not move between adsorbent and its medium is called as pH_{PZC} and as shown in Fig. 5, the pH_{PZC} obtained in this study is 6.37. This pH_{PZC} of Fe₃O₄-FA is smaller than that of bare Fe₃O₄, i.e. 8.2 as reported by El-Kharrag [14]. It may be caused by the fact that Fe₃O₄-FA contains carboxyl groups that the bare Fe₃O₄.

Qualitative Analysis of Magnetic Properties

Simple qualitative test for the magnetic properties of FA, Fe₃O₄ and Fe₃O₄-FA is performed by attracting the three materials with external magnetic field. As shown in Fig. 6, Fe₃O₄ and Fe₃O₄-FA but not FA were

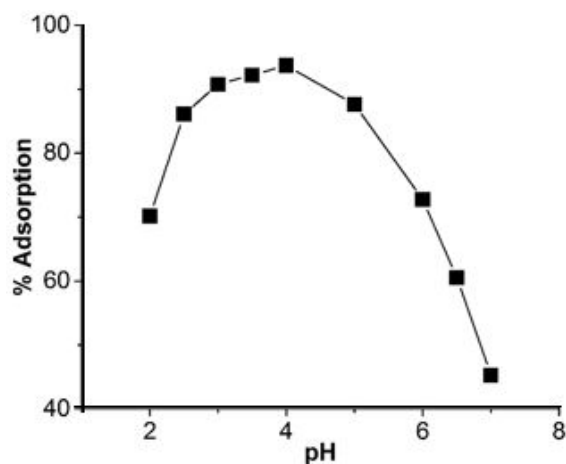


Fig 7. The effect of pH on adsorption of $[\text{AuCl}_4]^-$

attracted by magnet. It means that only Fe_3O_4 and $\text{Fe}_3\text{O}_4\text{-FA}$ have magnetic property. Attracted $\text{Fe}_3\text{O}_4\text{-FA}$ into external magnetic field indicated that coating of FA onto Fe_3O_4 surface was not remove the magnetic properties of Fe_3O_4 .

Sorption Process

Effect of the medium acidity on the adsorption of $[\text{AuCl}_4]^-$

The effect of the medium acidity on the adsorption of $[\text{AuCl}_4]^-$ on $\text{Fe}_3\text{O}_4\text{-FA}$ is given in Fig. 7. At very low pH (< 3.0), adsorbent system practically has less stability instead of pH > 3.0 . This means, with the decreasing pH from 3.0 to 2.0 lead to less percentage of adsorbed $[\text{AuCl}_4]^-$. At pH 4.0, fulvic acid protonated ($-\text{COOH}$) and lead to the complete adsorption with the negative species of $[\text{AuCl}_4]^-$ through hydrogen bonding. By increasing pH after 4.0, more functional groups of fulvic acid are deprotonated and more functional groups are negatively charged. This lead to the repulsion of negatively charged FA and $[\text{AuCl}_4]^-$, causing the percentage of adsorbed $[\text{AuCl}_4]^-$ decreased with the increasing pH.

Adsorption rate

The adsorption profile of $[\text{AuCl}_4]^-$ on $\text{Fe}_3\text{O}_4\text{-FA}$ as a function of interaction time is given in Fig. 8. The adsorption was initial rapid at first 90 min and then went slower. Based on the assumption that carboxyl group of fulvic acid is the responsible functional group for the binding with $[\text{AuCl}_4]^-$, the unit of adsorbed $[\text{AuCl}_4]^-$ in Fig. 8 has been converted from its original unit to mole unit based on the content of that carboxyl functional group. Among functional groups of FA, carboxyl plays important role to binding with $[\text{AuCl}_4]^-$ through electrostatic interaction. The determination of carboxyl content in FA

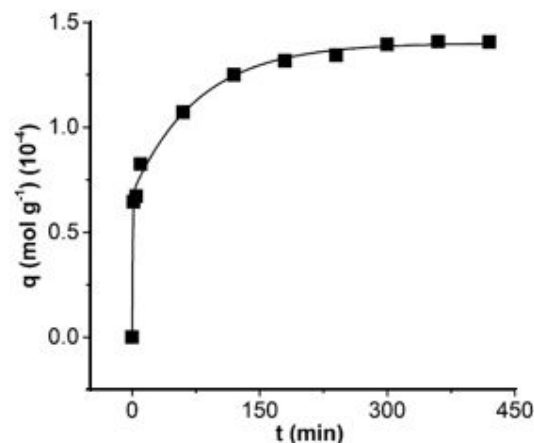


Fig 8. The effect of contact time on the adsorption of $[\text{AuCl}_4]^-$

used in this study using Ca-acetate method (Table 2) yielded the value of 6.78 mmol g^{-1} .

The determination of rate constant reveal that the sorption of $[\text{AuCl}_4]^-$ on $\text{Fe}_3\text{O}_4\text{-FA}$ obeys Ho's kinetic model as expressed in equation 1 [37].

$$\frac{t}{q_t} = \frac{1}{k_{\text{ads}} q_e^2} + \frac{1}{q_e} t \quad (1)$$

where q_e and q_t are the concentration (mol g^{-1}) of adsorbate at equilibrium and t , respectively. k_{ads} is the Ho rate constant of adsorption ($\text{g mol}^{-1} \text{ min}^{-1}$) and t is interaction time.

Plot of t/q_t against t from the data Fig. 8 gave a linier relationship with linearity (R^2) as high as 0.9983. Based on the slope of the plot, the obtained k_{ads} was $8 \times 10^3 \text{ g mol}^{-1} \text{ min}^{-1}$.

Adsorption capacity and energy

The adsorption profile of $[\text{AuCl}_4]^-$ on $\text{Fe}_3\text{O}_4\text{-FA}$ as a function of concentrations time is given in Fig. 9. The adsorption was rapid at initial concentration from 0 to 60 mg L^{-1} . The adsorption then increased slightly when the applied concentration of $[\text{AuCl}_4]^-$ was between 60 and 250 mg L^{-1} . The plot of C_e/q_e against C_e fitted to the linear form of Langmuir adsorption model as expressed in equation 2 [26].

$$\frac{C_e}{q_e} = \frac{1}{q_m K} + \frac{1}{q_m} C_e \quad (2)$$

where q_m is the adsorption capacity corresponding to complete monolayer coverage and K is the equilibrium constant (L mol^{-1}). The data fit well to the model with correlation coefficients (R^2) 0.9837, and the adsorption capacity of $1.24 \times 10^{-4} \text{ mol g}^{-1}$ for $[\text{AuCl}_4]^-$.

Monolayer coverage of the sorption $[\text{AuCl}_4]^-$ onto $\text{Fe}_3\text{O}_4\text{-FA}$ surface may indicate that only one functional group of fulvic acid is responsible for the adsorption. Although FA has many carboxyl and hydroxyl groups, it seems that only one group is dominant the adsorption

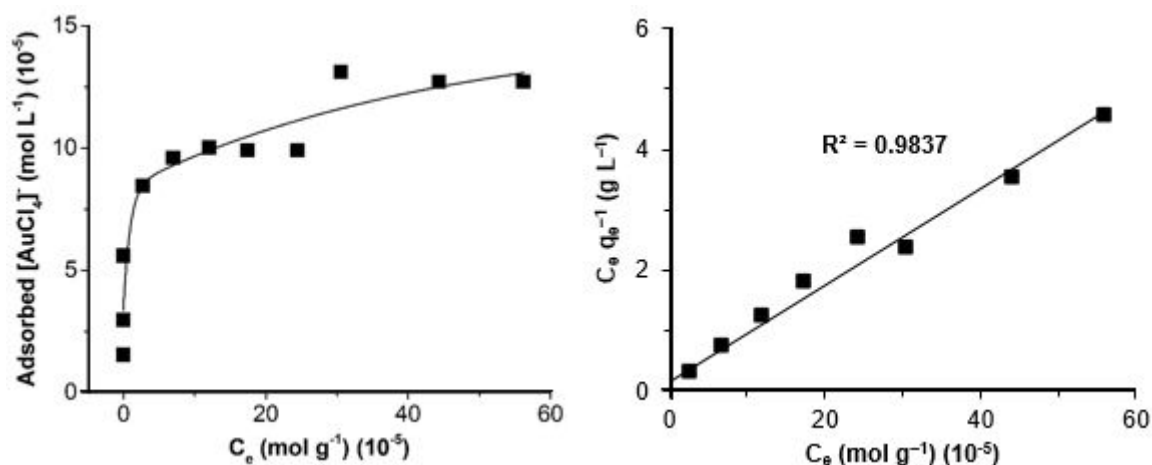


Fig 9. Relationship between adsorbed [AuCl₄]⁻ and the remaining concentration of [AuCl₄]⁻ in the solution at equilibrium (left), and linear form of Langmuir equation of adsorption of [AuCl₄]⁻ on Fe₃O₄-FA (right)

of [AuCl₄]⁻. There is a possibility that carboxyl group is the responsible functional group for the binding of [AuCl₄]⁻, while the content of -COOH on Fe₃O₄-FA used in this study was 67.8 cmol kg⁻¹ and equivalent to 6.78 mmol g⁻¹. This means, the adsorption capacity of Fe₃O₄-FA in adsorbing [AuCl₄]⁻ as high as 1.24 × 10⁻⁴ mol g⁻¹ will be equivalent to 0.124 mmol g⁻¹.

The value of equilibrium constant (K) can be determined from the intercept of plot C_e/q_e against C_e. The calculation showed that the value of K was 6.03 × 10⁴ L mol⁻¹. According to the equation E_{ads} = -ΔG_{ads}^o = RTlnK [38], the adsorption energy obtained is 27.27 kJ mol⁻¹.

Confirmation of the presence of reductive adsorption

FT-IR spectra confirmed that -COOH group was involved on the adsorption of [AuCl₄]⁻. Before adsorption, Fe₃O₄-FA shown main absorption bands originated from FA at 1627 cm⁻¹. Absorption band at 1627 cm⁻¹ was characteristic for stretching of aromatic C=C and stretching of C=O in COO⁻ [39].

After the adsorption of [AuCl₄]⁻, the intensity of the band at 1627 cm⁻¹ significantly increase, this might due to the formation of C=O of Ar=O as the result of the oxidation of phenolic group used for reducing [AuCl₄]⁻. Moreover, the intensity of the band at 3400 cm⁻¹ was decreased and might due to H atom of phenolic group had been released during the for reduction of [AuCl₄]⁻. The result of FT-IR agreed well with Hamamoto [35] that -OH of phenolic group has ability to reduce gold ion into gold metal as explained in the reaction below [40].



XRD patterns of Fe₃O₄-FA after adsorption confirm the presence of Au(0) through the appearance of peaks at 2θ: 37.41°; 43.66°; 64.25° and 76.67° that refers to face

Table 3. Medium acidity before and after adsorption-reduction process

pH	
Before	After
1.98	2.18
2.51	2.61
3.01	2.98
3.50	3.30
3.94	3.53
4.92	4.21
6.05	4.75
6.56	5.75
7.01	6.15

centered cubic crystal. Based on the reaction (1), can be explained that to reduce 1.0 mole of [AuCl₄]⁻, 3 moles of H⁺ from phenolic groups are needed. This also means that the reduction of 1.0 mole [AuCl₄]⁻ will produce 3 moles of Ar=O and H⁺. If it is assumed that gold is produced from the adsorbed [AuCl₄]⁻ by carboxyl group (0.124 mmol g⁻¹), it was needed 0.369 mmol g⁻¹ (three times of adsorbed [AuCl₄]⁻) of -OH content to reduce the adsorbed [AuCl₄]⁻ on Fe₃O₄-FA.

The released H⁺ increases the acidity of the medium as the result of reduction process. Table 3 confirm the decreasing pH after reductive adsorption process of [AuCl₄]⁻ into Au(0).

CONCLUSION

Fe₃O₄-FA was easily synthesized through a cheap and environmentally friendly preparation using iron salt by coprecipitation method using NH₄OH. The presence of FA lead to well dispersed and small particles of Fe₃O₄ (with 14.84 nm of Fe₃O₄ cores). The adsorbent stability and pHPZC affected the optimum pH of the adsorption. Adsorption of the [AuCl₄]⁻ was optimum at pH of 4 in which Fe₃O₄ was at its high

stability and positively charged. Sorption reached the equilibrium in 5 h and agreed well to Ho's kinetic model with rate constant (k) $8.0 \times 10^3 \text{ g mol}^{-1} \text{ min}^{-1}$ and followed Langmuir adsorption model with adsorption capacity $1.24 \times 10^{-4} \text{ mol g}^{-1}$.

ACKNOWLEDGEMENT

This study was supported by Bidikmisi Scholarship from Ministry of Education and Culture, Republic of Indonesia for the first author and *Penelitian Tim Pascasarjana* 2017, No. 2542/UN1.P.III/DIT-LIT/LT/2017 date April 19, 2017. This paper was dedicated to the late of Prof. Dr. Narsito of Chemistry Department, Universitas Gadjah Mada, for the supervision that enabling the first author to finish his Bachelor Degree.

REFERENCES

- [1] Birloaga, I., De Michelis, I., Ferella, F., Buzatu, M., and Vegliò, F., 2013, Study on the influence of various factors in the hydrometallurgical processing of waste printed circuit boards for copper and gold recovery, *Waste Manage.*, 33 (4), 935–941.
- [2] Kotte, P., and Yun, Y.S., 2014, L-cysteine impregnated alginate capsules as a sorbent for gold recovery, *Polym. Degrad. Stab.*, 109, 424–429.
- [3] Li, H., Wang, X., Cao, L., Zhang, X., and Yang, C., 2015, Gold-recovery PVDF membrane functionalized with thiosemicarbazide, *Chem. Eng. J.*, 280, 399–408.
- [4] Aylmore, M.G., and Muir, D.M., 2001, Thiosulfate leaching of gold: A review, *Miner. Eng.*, 14 (2), 135–174.
- [5] Pangen, B., Paudyal, H., Abe, M., Inoue, K., Kawakita, H., Ohto, K., Adhikaria, B.B., and Alam, S., 2012, Selective recovery of gold using some cross-linked polysaccharide gels, *Green Chem.*, 14, 1917–1927.
- [6] Villalobos, L.F., Yapici, T., and Peinemann, K.V., 2014, Poly-thiosemicarbazide membrane for gold recovery, *Sep. Purif. Technol.*, 136, 94–104.
- [7] Syed, S., 2012, Recovery of gold from secondary sources-A review, *Hydrometallurgy*, 115-116, 30–51.
- [8] Botz, M.M., Mudder, T.I., and Akcil, A., 2005, "Cyanide Treatment: Physical, Chemical and Biological Processes" in *Advances in Gold Ore Processing*, Adams, M., ed., Elsevier Ltd., Amsterdam, 672–700.
- [9] Fricker, A.G., 1993, Recovery of cyanide in the extraction of gold, *J. Cleaner Prod.*, 1 (2), 77–80.
- [10] Mudder, T.I., and Botz, M.M., 2004, Cyanide and society: A critical reviews, *Eur. J. Miner. Process. Environ. Prot.*, 4 (1), 62–74.
- [11] Yap, C.Y., and Mohamed, N., 2007, An electro-generative process for the recovery of gold from cyanide solutions, *Chemosphere*, 67 (8), 1502–1510.
- [12] El Ghandour, H., Zidan, H.M., Khalil, M.M.H., and Ismail, M.I.M., 2012, Synthesis and some physical properties of magnetite (Fe_3O_4) nanoparticles, *Int. J. Electrochem. Sci.*, 7, 5734–5745.
- [13] Sun, J., Zhou, S., Hou, P., Yang, Y., Weng, J., Li, X., and Li, M., 2006, Synthesis and characterization of biocompatible Fe_3O_4 nanoparticles, *J. Biomed. Mater. Res. Part A*, 80 (2), 333–341.
- [14] El-kharrag, R., Amin, A., and Greish, Y.E., 2011, Low temperature synthesis of monolithic mesoporous magnetite nanoparticles, *Ceram. Int.*, 38 (1), 627–634.
- [15] Lim, S.H., Woo, E.J., Lee, H., and Lee, C.H., 2008, Synthesis of magnetite-mesoporous silica composites as adsorbents for desulfurization from natural gas, *Appl. Catal., B*, 85 (1-2), 71–76.
- [16] Maity, D., and Agrawal, D.C., 2007, Synthesis of iron oxide nanoparticles under oxidizing environment and their stabilization in aqueous and non-aqueous media, *J. Magn. Magn. Mater.*, 308 (1), 46–55.
- [17] Zhang, L., He, R., and Gu, H.C., 2006, Oleic acid coating on the monodisperse magnetite nanoparticles, *Appl. Surf. Sci.*, 253 (5), 2611–2617.
- [18] Tan, K.H., 1998, *Principle of Soil Chemistry*, Marcel Dekker, New York.
- [19] Buhani, and Suharso, 2006, The influence of pH towards multiple metal ion adsorption of Cu(II), Zn(II), Mn(II), and Fe(II) on humic acid, *Indones. J. Chem.*, 6 (1), 43–46.
- [20] Narsito, Santosa, S.J., and Lastuti, S., 2008, Photo-reduction kinetics of MnO_2 in aquatic environments containing humic acids, *Indones. J. Chem.*, 8 (1), 37–41.
- [21] Nurmasari, R., Santosa, U.T., Umaningrum, D., and Rohman, T., 2010, Immobilization of humic acid on chitosan beads by protected cross-linking method and its application as sorbent for Pb(II), *Indones. J. Chem.*, 10 (1), 88–95.
- [22] Santosa, U.T., Mustikasaria, K., Santosa, S.J., and Siswanta, D., 2007, Study of sensitization of fulvic acid on photoreduction of Cr(VI) to Cr(III) by TiO_2 photocatalyst, *Indones. J. Chem.*, 7 (1), 25–31.
- [23] Umaningrum, D., Santosa, U.T., Nurmasari, R., and Yunus, R., 2010, Adsorption kinetics of Pb(II), Cd(II), and Cr(III) on adsorbent produced by protected-crosslinking of humic acid-chitosan, *Indones. J. Chem.*, 10 (1), 80-87.

- [24] Carlos, L., Einschlag, F.S.G., González, M.C., and Mártire, D.O., "Applications of Magnetite Nanoparticles for Heavy Metal Removal from Wastewater" in *Waste Water: Treatment Technologies and Recent Analytical Developments*, Eds. Einschlag, F.S.G., and Carlos, L., InTech, Croatia, 2013, 63–77.
- [25] Koesnarpadi, S., Santosa, S.J., Siswanta, D., and Rusdiarso, B., 2015, Synthesis and characterization of magnetite nanoparticle coated humic acid ($\text{Fe}_3\text{O}_4/\text{HA}$), *Procedia Environ. Sci.*, 30, 103–108.
- [26] Illés, E., and Tombácz, E., 2003, The role of variable surface charge and surface complexation in the adsorption of humic acid on magnetite, *Colloids Surf., A*, 230 (1-3), 99–109.
- [27] Illés, E., and Tombácz, E., 2006, The effect of humic acid adsorption on pH-dependent surface charging and aggregation of magnetite nanoparticles, *J. Colloid Interface Sci.*, 295 (1), 115–123.
- [28] Skogerboe, R.K., and Wilson, S.A., 1981, Reduction of ionic species by fulvic acid, *Anal. Chem.*, 53 (2), 228–232.
- [29] Jayaganesh, S., and Senthurpandian, V.K., 2010, Extraction and characterization of humic and fulvic acids from latosols under tea cultivation in South India, *Asian J. Earth. Sci.*, 3 (3), 130–135.
- [30] Liu, J.F., Zhao, Z.S., and Hang, G.B., 2008, Coating Fe_3O_4 magnetic nanoparticles with humic acid for high efficient removal of heavy metals in water, *Environ. Sci. Technol.*, 42 (18), 6949–6954.
- [31] Peng, L., Qin, P., Lei, M., Zeng, Q., Song, H., Yang, J., Shao, J., Liao, B., and Gu, J., 2012, Modifying Fe_3O_4 nanoparticles with humic acid for removal of Rhodamine B in water, *J. Hazard. Mater.*, 209-210, 193–198.
- [32] Niu, H., Zhang, D., Zhang, S., Zhang, X., Meng, Z., and Cai, Y., 2011, Humic acid coated Fe_3O_4 magnetic nanoparticles as highly efficient Fenton-like catalyst for complete mineralization of sulfathiazole, *J. Hazard. Mater.*, 190 (1-3), 559–565.
- [33] Petcharoen, K., and Sirivat, A., 2012, Synthesis and characterization of magnetite nanoparticles via the chemical co-precipitation method, *Mater. Sci. Eng., B*, 177 (5), 421–427.
- [34] Stevenson, F.J., 1994, *Humus Chemistry*, 2nd ed., John Wiley and Sons., New York, 512.
- [35] Laurent, S., Forge, D., Port, M., Roch, A., Robic, C., Vander Elst, L., and Muller, R.N., 2008, Magnetic iron oxide nanoparticles: Synthesis, stabilization, vectorization, physic chemical characterizations and biological applications, *Chem. Rev.*, 108 (6), 2064–2110.
- [36] Hasnah, S.D., and Ridwan, 2012, Sintesis dan Karakterisasi Nanopartikel Fe_3O_4 Magnetik untuk Adsorpsi Kromium Heksavalen, *JUSAMI*, 13 (2), 136–140.
- [37] Ho, Y.S., 2006, Review of second-order models for adsorption systems, *J. Hazard. Mater.*, 136 (3), 681–689.
- [38] Santosa, S.J., Sudiono, S., and Shiddiq, Z., 2007, Effective humic acid removal using Zn/Al layered double hydroxide anionic clay, *J. Ion Exchange*, 18 (4), 322–327.
- [39] Santosa, S.J., Siswanta, D., Sudiono, S., and Utarianingrum, R., 2008, Chitin-humic acid hybrid as adsorbent for Cr(III) in effluent of tannery wastewater treatment, *Appl. Surf. Sci.*, 254 (23), 7846–7850.
- [40] Hamamoto, K., Kawakita, H., Ohto, K., and Inoue, K., 2009, Polymerization of phenol derivatives by the reduction of gold ions to gold metal, *React. Funct. Polym.*, 69(9), 694–697.